Suppression of Cavity Formation in Ceramics: Prospects for Superplasticity

A. G. EVANS*

Materials Department, University of California at Berkeley, Berkeley, California 94720

J. R. RICE

Division of Engineering, Brown University, Providence, Rhode Island 02912

J. P. HIRTH

Metallurgical Engineering Department, Ohio State University, Columbus, Ohio 43210

Ceramics exhibit macroscopic stress/strain rate relations that should lead to superplastic extension. However, premature fracture is normally encountered, due to the formation and growth of grain-boundary cavities. Thus, cavity nucleation and growth were analyzed in an attempt to identify microstructures and/or strain-rate regimes that would suppress cavity evolution and hence allow superplasticity. Analysis of cavity nucleation indicates that fine-grained materials devoid of grain-boundary amorphous phases and inclusions should sustain substantial deformation rates without nucleating cavities, especially if solid-solution additions that encourage rapid grain-boundary diffusion (while not excessively decreasing surface energy) are identified. The analysis of void growth indicates that high relative surface diffusivities are also desirable, indicating that alloy additions that do not depress (and probably enhance) the relative surface diffusivities must be selected.

I. Introduction

WHEN polycrystalline ceramic materials are deformed in tension at high temperatures, cavity formation and growth are prevalent.[1,2] The cavities substantially limit the fracture strains and prevent the application of potentially viable deformation-forming techniques (e.g. superplastic forming). The mode of formation and initial propagation of these cavities is evaluated in the present paper, to identify the material parameters that are primarily responsible for cavity evolution. Concepts for microstructural modifications that would suppress cavity evolution at strain rates of practical interest are then proposed.

Cavities can be generated at grain boundaries if the local stress exceeds the interface rupture strength or if vacancies can coalesce into a size that exceeds a critical nucleation size. The propensity for cavity formation is, in both cases, affected by the presence of stress concentrations. The origin and character of the most severe sources of elastic stress concentration and their relaxation by diffusion are thus examined before detailing the cavity formation and growth concepts.

II. Stress Concentrations

The two primary sources of appreciable stress concentration in ceramics at high temperatures are thermal-expansion anisotropy and, when subjected to a tensile stress, grain-boundary sliding. The development of elastic stress concentrations and their partial relaxation by diffusion processes are examined separately for both sources.

(1) Boundary Sliding

When a remote stress σ_∞ is applied to a polycrystal, boundary sliding occurs with a relatively short relaxation time* to generate stress singularities on adjacent boundaries (Fig. 1). The magnitude of this singularity depends on the deformation properties of the material.[4] For most polycrystalline ceramics, the grains can be assumed to respond in a linear elastic mode and the boundaries in a linear viscous fashion. For this case, bounds on the singularity can be obtained from a two-dimensional solution for a polygon array with completely relaxed grain boundaries[4]:

$$\sigma \leq 0.41 \; \sigma_\infty \sqrt{d/x} \equiv \kappa_u / \sqrt{x} \tag{1a}$$

where σ is the local stress, d the grain facet length, and x the distance from the triple point. From the solution for the tensile stress concentration of a single mode II penny-shaped crack[5] (loaded by the shear $\sigma_\infty/2$),

$$\sigma \geq 0.18\sigma_\infty \sqrt{d/x} \equiv \kappa_L / \sqrt{x} \tag{1b}$$

These high local tensile stresses cause matter to diffuse to adjacent (less stressed) boundaries and the stress singularity disappears, as indicated by the dashed line in Fig. 1. The relaxed stress distribution can be estimated for an infinite bicrystal (Fig. 2), with the assumption that the time-dependent stress distribution $\sigma(x,t)$ has the form at $t=0$ suggested by Eq. (1), viz.:

$$\sigma(x,0) = \begin{cases} \kappa/\sqrt{x} & x>0 \\ 0 & x<0 \end{cases} \tag{2}$$

This stress distribution can be modeled by inserting a continuous distribution of opening dislocations along the negative x axis, with the density of the distribution proportional to $1/\sqrt{-x}$.[6,7,†]

If $\delta = \delta(x,t)$ is the effective "thickening" of the grain boundary (caused by the addition of matter to the crystals on each side) and J is the number of atoms diffusing along the grain boundary‡ per unit time, per unit thickness into the plane of the diagram, mass conservation requires that

$$\Omega \partial J / \partial x + \partial \delta / \partial t = 0 \tag{3}$$

Further, the linearized law of diffusion is[6,10]

$$\Omega J = -\frac{D_b \delta_b}{kT} \frac{\partial}{\partial x}(-\Omega \sigma) \tag{4}$$

where the equation has been arranged to emphasize that $-\Omega\sigma$ is the chemical potential per atom. Here $D_b\delta_b$ is the grain-boundary diffu-

---

---

*For example, the ratio of the relaxation time for sliding to that for boundary diffusion in the presence of a viscous boundary phase is $\approx 60\pi d^2/\Omega^{2/3}$, where Ω is the atomic volume and d is the grain-facet length (Ref. 3).

†Alternatively, the matter flow from the stressed boundary can be seen as causing the climb of discrete grain-boundary dislocations near the triple junction producing a climb pileup configuration. The pileup stress superposes on and relaxes the concentrated stress (Fig. 1). Differences in the continuous and discrete dislocation descriptions appear only over distances of the order of the grain-boundary dislocation spacing, in accord with St. Venant's principle.

‡The principal diffusion path in the present analysis is considered to be along grain boundaries, which is true if $D_b\delta_b \gg D_l\lambda$, where D_l is the lattice diffusivity and λ is the characteristic interval in x over which diffusion is occurring. For the present situations, this condition should invariably be satisfied on the basis of typical values for D_b and D_l (Refs. 8 and 9).

Fig. 2. Bicrystal system used to model diffusional relaxation of sliding singularity in Fig. 1.

Fig. 3. Initial and relaxed stress distribution plotted using normalized coordinates suggested by the analysis.
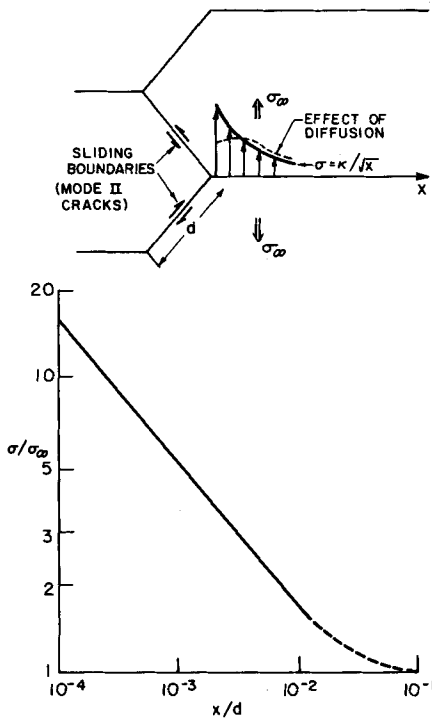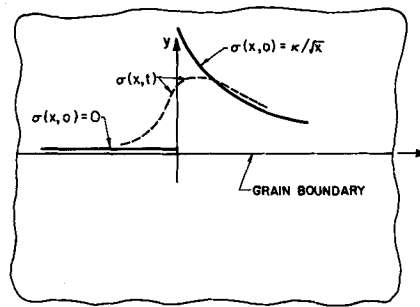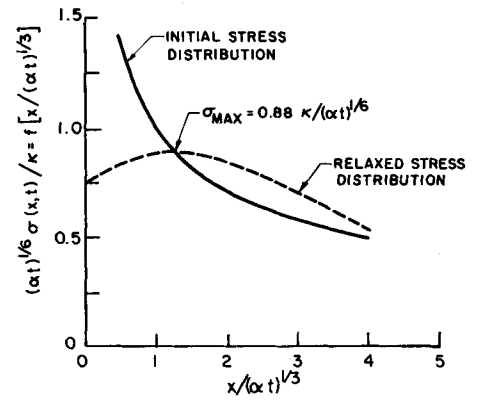
Fig. 1. Tensile stresses developed as a result of freely sliding grain boundaries.

sion parameter, with D_b the grain-boundary diffusivity and δ_b the effective width of the boundary. Hence,

$$(D_b\delta_b\Omega/kT)(\partial^2\sigma/\partial x^2)+(\partial\delta/\partial t)=0 \tag{5}$$

A standard result of plane-strain isotropic elasticity indicates that for a stress distribution

$$\sigma(x,t)=B(t)e^{i\omega x} \tag{6}$$

where B contains the time dependence of the stress acting along the x axis, the required distribution of the thickening displacement δ is twice the surface displacement in the corresponding problem of load application to a half-space. Thus, following Chuang[6] and Chuang *et al.*[11]

$$\delta(x,t)=-[2(1-\nu)/G|\omega|]B(t)e^{i\omega x} \tag{7}$$

where G is the elastic shear modulus and ν the Poisson ratio. If the expressions for σ and δ are to satisfy the diffusion equation (Eq. (5)), a necessary condition is

$$B(t)=B_0 \exp[-\alpha|\omega^3|t] \tag{8}$$

where[11]

$$\alpha=GD_b\delta_b\Omega/2(1-\nu)kT \tag{9}$$

Hence, if the initial stress distribution of Fig. 2 is represented by

$$\sigma(x,0)= \int_{-\infty}^{+\infty} B_0(\omega)e^{i\omega x}d\omega \tag{10}$$

the stress distribution at any time $t>0$ is

$$\sigma(x,t)= \int_{-\infty}^{+\infty} B_0(\omega) \exp[-\alpha|\omega^3|t]e^{i\omega x}d\omega \tag{11}$$

Fourier inversion of Eq. (11) and a straightforward integration based on the form for $\sigma(x,0)$ given earlier yields the result

$$B_0(\omega) = (1/2\pi)\int_{-\infty}^{+\infty}\sigma(x,0)e^{-i\omega x}dx \tag{12a}$$

$$= (\kappa/2\pi)\int_0^{+\infty} x^{-1/2}e^{-i\omega x}dx \tag{12b}$$

$$=\begin{cases} \kappa(1-i)/2\sqrt{2\pi}|\omega|^{1/2} & \omega>0 \\ \kappa(1+i)/2\sqrt{2\pi}|\omega|^{1/2} & \omega<0 \end{cases} \tag{12c}$$

When these results are inserted into the integral for σ (x,t) (Eq. (11)), and $\omega=u^2/(\alpha t)^{1/3}$ is substituted, the result is

$$\sigma(x,t)=[\kappa/(\alpha t)^{1/6}]f[x/(\alpha t)^{1/3}] \tag{13}$$

where

$$f[Z]= \sqrt{\frac{2}{\pi}}\int_0^{\infty} \exp(-u^6)[\cos(u^2Z)+\sin(u^2Z)]du \tag{14}$$

The function $f[Z]$ approaches $Z^{-1/2}$ at large Z, so that the classical elastic stress distribution remains (for a short enough time) at points far removed from the grain junction. But, $f[0]=0.74$, and hence the stress at the junction, for $t>0$, is

$$\sigma(0,t)=0.74[\kappa/(\alpha t)^{1/6}] \tag{15}$$

Indeed, $(\alpha t)^{1/3}$ is the measure of the distance from the grain junction over which the stress concentration is seriously mitigated by diffusion (Fig. 3). The maximum stress is

$$\sigma_{max}=0.88[\kappa/(\alpha t)^{1/6}] \tag{16}$$

which occurs at approximately $x=1.3(\alpha t)^{1/3}$. The result corresponds approximately to calculating σ_{max} as the initial stress acting at the distance $1.3(\alpha t)^{1/3}$ from the grain junction.

This solution pertains to a stress field $\kappa/\sqrt{x}$ that has been created by instantaneous load application. If, instead, κ is some continuous function of time, say $\kappa=\kappa(t)$, representing the time dependence of external loadings exerted on the polycrystal with freely slipping boundaries, then by standard superposition techniques

$$\sigma(x,t)= \int_{-\infty}^{t} \frac{d\kappa(t')/dt'}{\alpha^{1/6}(t-t')^{1/6}}f\left[\frac{x}{\alpha^{1/3}(t-t')^{1/3}}\right]dt' \tag{17}$$

In particular, the stress σ $(0,t)$ at the junction can be calculated, using $f[0]=0.74$. If the load increases linearly in time, starting at $t=0$, equivalent to a constant rate $\dot{\kappa}$ of stress intensity, the stress at the junction would be

$$\sigma(0,t)=0.89[\dot{\kappa}t/(\alpha t)^{1/6}] \tag{18a}$$

On the basis of the plot in Fig. 3, the maximum stress in the specimen might exceed this value by $\approx 10\%$. Hence, if this maximum admissible stress level for the grain junction is known, the maximum permissible loading rate $\dot{\kappa}$ can be estimated.

For example, consider

$$\sigma_{max} \approx [\kappa/(\alpha t_L)^{1/6}] \tag{18b}$$

as the maximum stress generated near the junction when loads equivalent to a stress intensity κ are applied at a uniform rate over a loading time t_L. If σ_{max} is not to exceed some critical stress level σ_c for fracture nucleation, the loading time must be long enough to satisfy

$$t_L \geqslant 4.8 \times 10^{-3} (\sigma_{\infty}/\sigma_c)^6 (d^3/\alpha) \quad \text{(upper bound)} \tag{19a}$$

$$t_L \geqslant 3.4 \times 10^{-5} (\sigma_{\infty}/\sigma_c)^6 (d^3/\alpha) \quad \text{(lower bound)} \tag{19b}$$

Note that, since the term $\exp(-\alpha|\omega^3|t)$ arises in the expression for decay of an initial stress (or thickening) distribution of spatial circular frequency ω, the term d^3/α of Eq. (19) can be interpreted as the grain-boundary relaxation time for disturbances of frequency $\omega = 1/d$.

It is instructive to examine the loading times t_L associated with the development of stress concentrations of magnitude 10 and 3 in typical ceramic systems. The most extensively documented systems are Al_2O_3 materials, in which the boundary diffusivities are[8]:

$$D_b \delta_b \approx 10^{-9} \exp[-Q/RT] m^3 \ s^{-1} \tag{20}$$

where Q is 400 kJ/mol. Values of t_L between the upper- and lower-bound solutions are plotted in Fig. 4, as a function of grain size, for the lowest temperatures at which significant deformation rates can be achieved, i.e. $\approx 1400°C$.[8] Evidently, except for coarse-grained materials, these large stress concentrations develop at much less than typical loading times. Hence, significant stress concentrations produced by boundary sliding are not expected to develop near triple points in high-strength aluminas unless rapid transients created by local instabilities can occur. The maximum stress in these materials caused by nontransient sliding is thus $2\sigma_{\infty}$, occurring at the centers of the grain facet in the fully relaxed condition.[10] Raj[12] estimated the time dependence for achievement of this fully relaxed condition. Boundary-diffusion rates have not been measured directly for highly covalent ceramics such as Si_3N_4 and SiC, but approximate values can be derived from creep or hot-pressing data. For hot-pressed Si_3N_4 (Ref. 9):

$$D_b \delta_b \approx 6 \times 10^{-4} \exp[-Q/RT] m^3 \ s^{-1} \tag{21}$$

where Q is 680 kJ/mol. Values of t_L at 1400°C are plotted in Fig. 4. These results indicate that, for typical experimental loading times, stress concentration factors of ≈ 3 should develop. The maximum achievable internal stress concentration for these materials should thus be taken as $\approx 3\sigma_{\infty}$, again with the assumption that local sliding transients do not develop. The stresses that develop at other temperatures, or in other materials, can be much larger.

(2) Thermal-Expansion Anisotropy

Polycrystalline ceramics with thermal-expansion anisotropy develop large stresses near grain triple points at temperatures below the fabrication temperature.[13] The stresses near the triple points, in the absence of diffusional relaxation, take the form:

$$\sigma_x \approx 0.24G \Delta\alpha\Delta T \ \ln(0.82d/x) \tag{22}$$

where x is the distance from the triple point, $2\Delta\alpha$ is the difference between the maximum and minimum thermal-expansion coefficients, and ΔT is the temperature differential between the ambient and fabrication temperatures. The steepness of the stress gradient suggests (cf. the sliding singularity Eq. (1)) that the stresses near the triple points should relax very rapidly at temperatures where appreciable grain-boundary diffusion can occur. The stresses along the grain facet should thus quickly tend toward the steady-state parabolic distribution typical of uniform thickening. The magnitude of the peak stress at the facet center should decrease continuously with time by vacancy migration from facets under tension to adjacent facets under compression.

The stress distribution along grain facets under conditions of uniform thickening can be found directly by integrating Eq. (5) as:

$$\sigma = (-x^2 \dot{\varepsilon} d/2\sqrt{2})(kT/\Omega D_b \delta_b) + C_1 x + C_2 \tag{23}$$

where $\dot{\varepsilon}$ is the rate of strain decrease associated with boundary thickening ($\dot{\varepsilon} = (\sqrt{2}/d)\dot{\delta}$) and C_1 and C_2 are constants. Inserting the (symmetry) boundary condition $d\sigma/dx = 0$ at $x = d/2$ and, for simplicity,* setting $\sigma = 0$ at $x = 0$ (cf. the analogous viscous liquid problem[14]) then gives:

$$\sigma = (\dot{\varepsilon} d/2\sqrt{2})(kT/\Omega D_d \delta_b)x(d-x) \tag{24}$$

The average stress $\langle\sigma\rangle$ along the facet is thus:

$$\langle\sigma\rangle = (d^3\dot{\varepsilon}/12\sqrt{2})(kT/\Omega D_b \delta_b) \tag{25}$$

and the maximum stress $\hat{\sigma}$ is $15 \ \langle\sigma\rangle$.

Noting that $\langle\sigma\rangle = 2G\varepsilon(1+\nu)$ and equating the initial strain to the unrelaxed strain, $2G\Delta\alpha\Delta T$, then gives the time t dependence of the maximum stress at constant temperature:

$$\hat{\sigma}(t) = 3G\Delta\alpha\Delta T \ \exp\left[-\left(\frac{24\sqrt{2}\Omega D_b \delta_b G(1+\nu)}{d^3 kT} \right) t \right] \tag{26}$$

Some typical stresses for polycrystalline alumina ($D_b \delta_b$ given by Eq. (20)) are plotted in Fig. 5. For test temperatures $>1400°C$, the thermal mismatch stresses relax very rapidly, especially in fine-grained materials. Their contribution to cavity formation in the materials of present interest is thus considered to be negligible.

III. Cavity Nucleation

The conditions of principal interest for the present analysis, i.e. those that involve appreciable grain-boundary diffusion, should limit the peak stress enough that the possibility of brittle grain-boundary cracking can be largely excluded, although this mode of crack nucleation should not be discounted under other test conditions. Cavity nucleation by vacancy coalescence is thus considered as the major mode of boundary separation. The formation of a cavity by vacancy coalescence can be derived by considering the changes in external work, surface energy, vacancy concentration, and strain energy that accompany introduction of the cavity. In the absence of strain-energy terms and surface-energy anisotropy the critical nucleus will have the form indicated in Fig. 6 and its energetics can be described by the methods of Raj[15] and Raj and Ashby.[16] In general, the strain-energy term is expected to be small for typical dimensions of the critical nucleus. However, strain-energy effects may not always be negligible and bounds on the role of strain energy are included in the following results (a related discussion is presented in Appendix I).

As indicated in Fig. 6, we treat the case of nucleation on a planar boundary, equilibrated with the local normal stress acting on the boundary prior to cavity nucleation, and with isotropic surface energy. On the basis of typical nucleation treatments,[17] anisotropic surface-energy considerations would have a minor modifying result through a geometric factor. Nonequilibrium conditions represented by a nonuniform distribution of grain-boundary dislocations (i.e. in the pileup configuration discussed previously (Section II(1)), would lead to a local enhancement of nucleation rate. Similarly, the presence of steps or offsets in the boundary would yield a local enhancement, analogous to other forms of nucleation.[18,19] Thus, the case treated here is a lower bound on nucleation effects. It can be readily shown from the change in Helmholtz free energy of the system[15,16] that the critical nucleation radius, r^*, is :

$$r^* = \frac{2\gamma_s}{\sigma_{\infty}[1 + 4\beta\sigma_{\infty} \sin^3\alpha/E\pi\zeta]} \tag{27}$$

where β is a constant ($0 \leq \beta \leq 1$) that depends on the elastic stress redistribution around the cavity, around vacancies, and at external surfaces (some issues related to the magnitude of the elastic field that dictates β are presented in Appendix I), γ_s is the surface energy, and $\zeta = 2 - 3 \cos\alpha + \cos^3\alpha$, where α is the equilibrium angle at the cavity/boundary intersection.

Plots of $r^*\sigma_{\infty}/\gamma_s$ as a function of α for several values of σ/E (assuming upper and lower bounds for β of unity and zero, respec-

---

*The exact boundary condition at $x = 0$ depends on the relative grain-boundary orientations at the triple point.
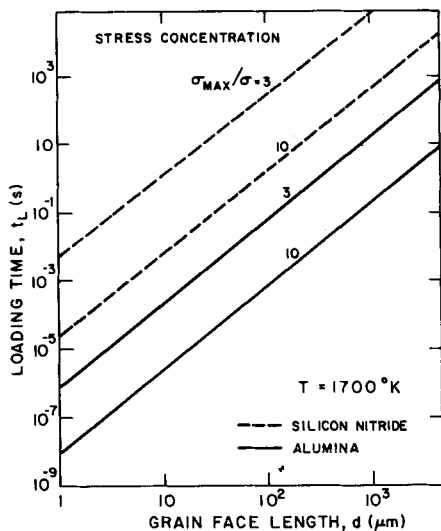
Fig. 4. Plot indicating grain-size dependence of loading time required to develop stress concentrations of 10 and 3 in Al_2O_3 and Si_3N_4.
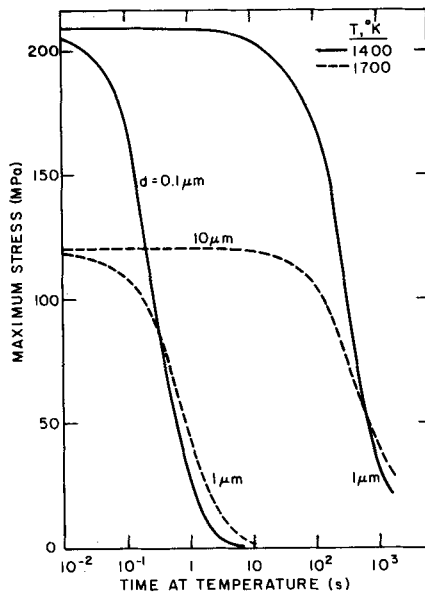

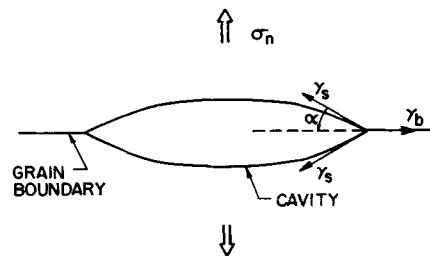**Fig. 5.** Plot of rate of diffusional relaxation of thermal-expansion-mismatch stresses in alumina.

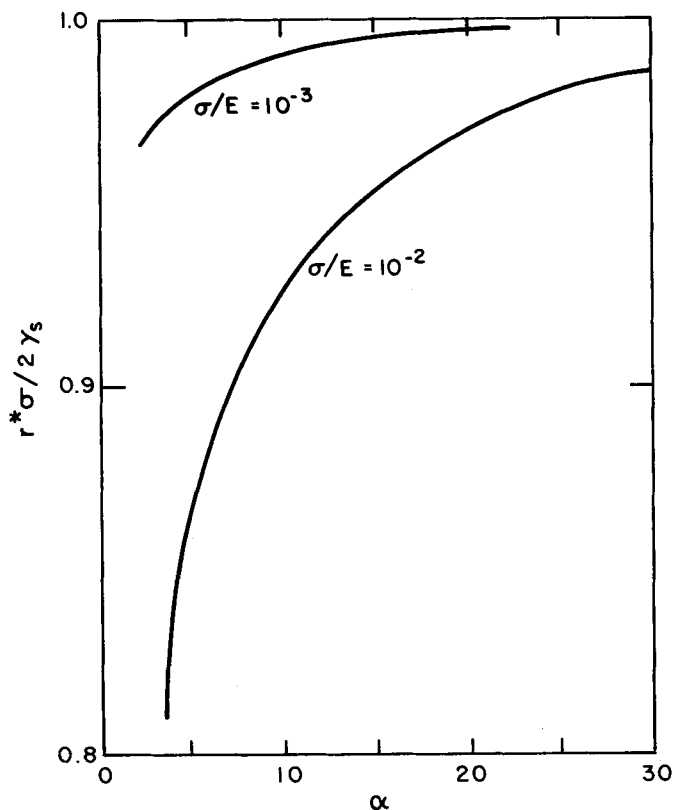**Fig. 6.** Geometry of double spherical cap-shaped nucleus.

Fig. 7. Effect of included angle, α, on size of critical nucleus obtained assuming an unrelaxed elastic stress field.
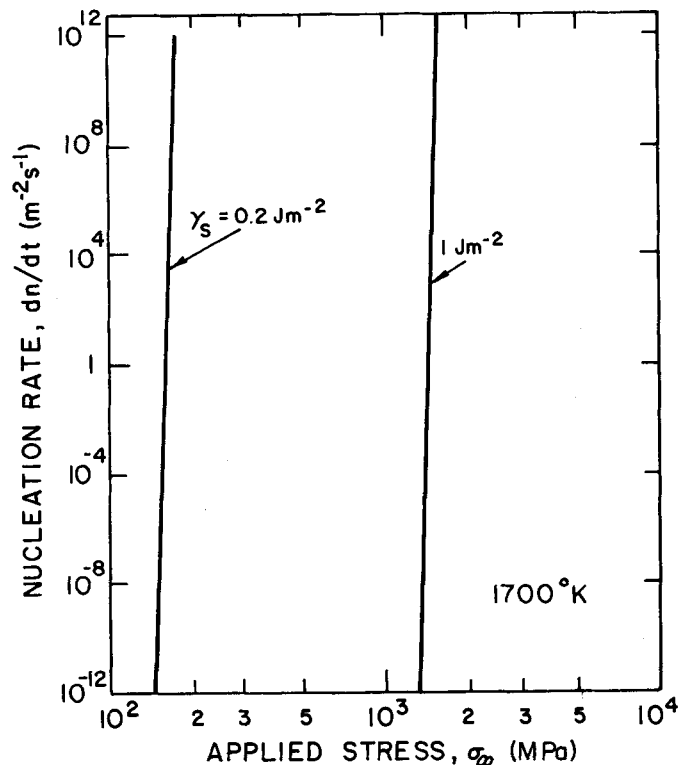

Fig. 8. Stress dependence of void nucleation rate at 1400°C for values of surface energy indicated.

tively) indicate (Fig. 7) that the strain-energy term can be important only for $\alpha \lesssim 20°$, i.e. boundary energies $\gamma_b \gtrsim 1.88\gamma_s$. This value of α is smaller than that typically expected for most polycrystalline ceramics (Appendix II). The strain-energy term can thus be neglected for most purposes (inclusions with a large interface energy may be an important exception).

Standard nucleation theory[17,19] now indicates that the nucleation rate, $\dot{n}$, (being the product of the number of nuclei at the critical size

and the probability that a vacancy will be added to a critical nucleus) is given by

$$\dot{n} = z(4\pi\gamma_s \sin\alpha/\sigma_\infty \Omega^{4/3})\mathcal{D}_b\delta_b n_0 \exp[-(4\pi\gamma_s^3\zeta/3\sigma_\infty^2 kT)] \quad (28)$$

where z is Zeldovich's factor ($\approx 10^{-2}$) and n_0 is the number of available nucleation sites per unit area of grain boundary. The nucleation rate exhibits a maximum at $\sigma_\infty^2 = 16\pi\gamma_s^3\zeta/3kT$. Stresses below the maximum are those that generally dictate nucleation. The stress dependence of the nucleation rate at stresses in this range is plotted in Fig. 8 for two values of the surface energy (0.2 J m^{-2} for
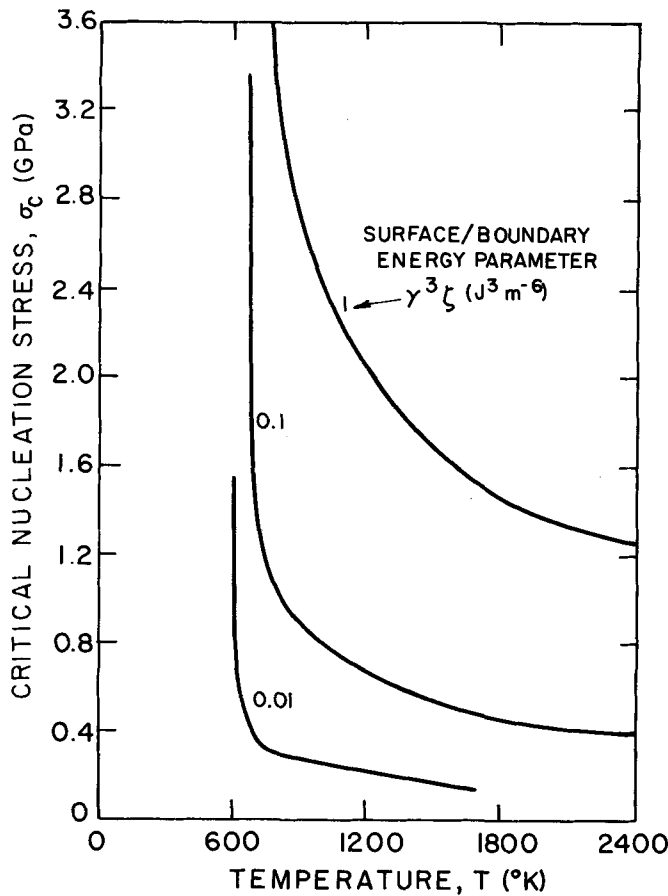
Fig. 9. Temperature dependence of "critical" void nucleation stress in alumina for values of surface/boundary energy parameter, $\zeta\gamma_s^3$, indicated.

Fig. 10. Plot of void length dependence of void growth rate at constant applied stress and constant surface diffusivity.

glass at high temperature, 1 J m^{-2} for most oxide ceramics at 1400°C using $\gamma_b \simeq \gamma_s$ (Appendix II), a typical $D_b\delta_b$ from Eq. (20), a grain size of 3 μm, and regarding all boundary sites as potential nucleation sites. It is evident that the large value of the formation energy leads essentially to "threshold" behavior, i.e. a critical stress, σ_c, for cavity nucleation. The critical stress is given by[*]:

$$\sigma_c^2 \simeq \frac{8\pi\gamma_s^3\zeta}{3kT \; \ln[4\pi z(\gamma_s\sin\alpha)D_b\delta_b \; n_0/\sigma_c\Omega^{4/3} \, \dot{n}]} \tag{29}$$

The temperature dependence of the nucleation stress in alumina,[†] obtained by letting $\dot{n} = 1$ m^{-2} s^{-1}, is plotted in Fig. 9 for several $\gamma_s^3\zeta$ (the variable that represents the boundary/surface energy influence on the nucleation process). For a $\gamma_s^3\zeta$ typical of polycrystals with clean grain boundaries, ≈ 1 J^3 m^{-6} (i.e. no glassy phase and no inclusions), local stresses >1 GPa are needed to initiate cavities. However, in the presence of an amorphous boundary phase, $\gamma_s^3\zeta$ is typically 0.03 J^3 m^{-6} ($\gamma_s \approx 0.2$ J m^{-2}) and local stresses <200 MPa are sufficient to nucleate cavities. In addition, heterogeneous cavity nucleation at inclusions will be possible if the inclusions have high interface energies (i.e. $\gamma_s^3\zeta$ values <0.03), especially when the inclusions coincide with the zones of stress concentration produced by boundary sliding.

IV. Cavity Propagation

The initial growth of a void is typically a quasi-equilibrium process,[11] wherein surface diffusion is rapid enough that the void shape remains invariant. Additionally, for the problem of present concern (initial growth after nucleation) the void spacing should be

much larger than the void length. For this condition the growth rate is given by[16,11]:

$$\frac{\dot{a}kT}{\Omega D_b\delta_b\gamma_s} \simeq \frac{[\sigma_\infty a/\gamma_s - 2\sin\alpha]\sin^3\alpha}{a^3 \; \ln \; (b/2a)\zeta} \tag{30}$$

where $2a$ is the cavity diameter and $2b$ is the separation between cavities. However, a transition to a different growth rate regime occurs at[11]

$$\dot{a}_c kTa^3/\Omega D_s\delta_s\gamma_s \simeq 24 \tag{31}$$

where $D_s\delta_s$ is the surface diffusion parameter. This transition coincides with the condition wherein the surface diffusion is too slow to retain the equilibrium shape of the cavity and a "cracklike" cavity develops. The growth rate in the crack-like regime is:

$$\left(\frac{\dot{a}kT}{\Omega D_s\delta_s\gamma_s}\right)^{1/3} = \frac{3\{[1 + 4Q\Delta\sigma_\infty b/3\gamma_s \; \sin(\alpha/2]^{1/2} - 1\}}{4b\Delta Q[1 - (a/b)^2]} \tag{32}$$

where $\Delta = D_s\delta_s/D_b\delta_b$ and

$$Q = 3(a/b)\{\ln \; (b/a) - 3/4 + (a/b)^2$$
$$[1 - (a/2b)^2 -]\}/[1 - (a/b)^2]^3 \tag{33}$$

At typical stress levels and for $\Delta \gg 1$, the term containing σ_∞ is much greater than unity[11] and Eq. (32) reduces to

$$\frac{\dot{a}kT}{\Omega D_b\delta_b\gamma_s} \simeq \frac{1}{[1 - (a/b)^2]^3}\left[\frac{3\sigma_\infty}{4Q\gamma_s b \; \sin(\alpha/2)}\right]^{3/2} \left(\frac{D_b\delta_b}{D_s\delta_s}\right)^{1/2}$$

$$\simeq 1.8 \left[\frac{\sigma_\infty}{\gamma_s b \; \sin(\alpha/2)}\right]^{3/2} \left(\frac{D_b\delta_b}{D_s\delta_s}\right)^{1/2} \tag{34}$$

where the numerical factor 1.8 is accurate to within ±17% for 0.1 < a/b < 0.4 (the factor becomes larger for a/b < 0.1 or > 0.4).

The void growth characteristics implied by Eqs. (30) and (34) are that the void grows transiently in the quasi-equilibrium mode (Eq. (30)) until eventually $a^3\dot{a}$ becomes too large for surface diffusion to maintain the spherical-cap shape. Thereafter, there is a gradual transition to growth in the cracklike mode, for which the limiting velocity depends primarily on D_b and D_s. The transition from one mode to the other occurs essentially when the average of the predicted growth rate expressions satisfies Eq. (31). Figure 10 shows schematically the growth rate $\dot{a}$ vs a under constant applied stress; $\dot{a}$

---

*σ_c is insensitive to small changes in the logarithmic term and it can be calculated accurately enough by letting the σ_c term in the parentheses be $\approx$ 100 MPa.

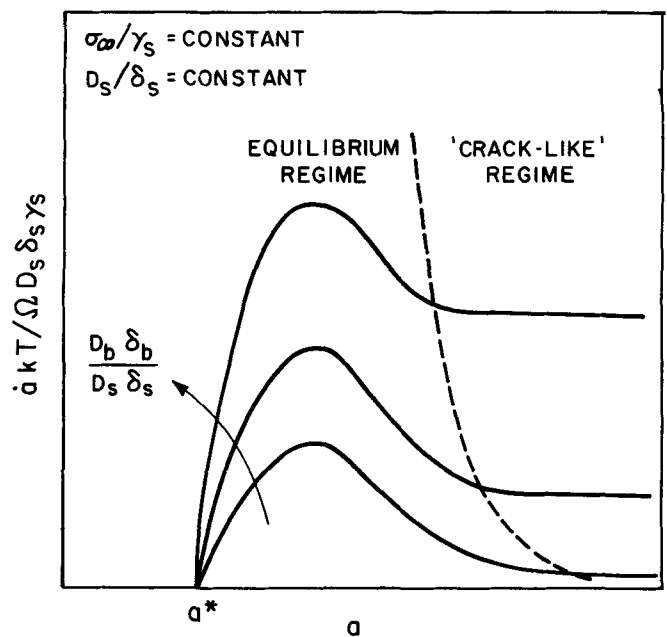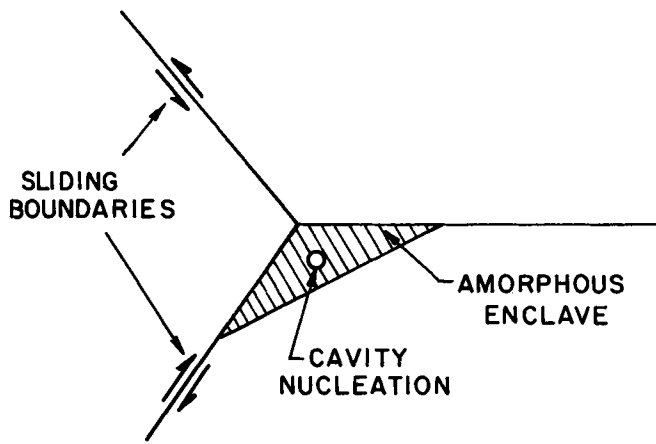†The result is insensitive to the grain size in the range 1 to 200 μm.

Fig. 11. Schematic of amorphous enclave typical of anisotropic ceramics, indicating cavity nucleation.

initially accelerates to a peak growth rate, dictated by σ_∞, γ_s, $D_b\delta_b$, and T, and then decelerates to an essentially constant steady-state level. The steady-state rate exhibits a dependence on $D_s\delta_s$, in the sense that the growth rate increases as the relative surface-diffusion rate decreases. An important feature of the void growth problem thus relates to the boundary and surface diffusivities of the polycrystal. In particular, low ratios of the surface-to-boundary diffusivity are of concern.

V. Discussion

(1) Cavity Suppression

As indicated in the preceding analysis, the most favorable sites for cavity formation in ceramic polycrystals are at triple points. The incidence of cavity formation can be assessed by comparing the relations for the local stress amplitude (Eqs. (18)) and the critical nucleation stress (Eq. (29)). The local stress amplitude of interest will be that required to produce deformation strain rates of practical use (e.g. $>10^{-3}$ s^{-1}). Typically, without cavity formation, the appropriate process controlling the steady-state strain rate will be boundary diffusion-controlled creep,[20] which yields a strain rate:

$$\dot\varepsilon = 10^2 \Omega D_b \delta_b \sigma_\infty / d^3 kT \qquad (35)$$

where d is now the grain diameter (mean linear intercept). Also, combining Eq. (35) with Eq. (18b) gives

$$t_L \dot\varepsilon \approx 10^{-2} (\sigma_\infty/E)(\sigma_\infty/\sigma_{max})^6 \qquad (36)$$

indicating that the local stress concentration bears a simple relation to the product of the steady-state strain rate and the loading time. Then, with the condition that the maximum stress cannot exceed the critical nucleation stress, Eqs. (29), (35), and (36) yield an expression for the strain rates that can be achieved without cavity formation near triple points:

$$\dot\varepsilon t_L^{-1/6} \lesssim 10^3 \left[\frac{\gamma_s^3 \zeta}{\ln(4\pi z \gamma_s \sin\alpha\, D_b\delta_b n_0/\sigma\Omega^{4/3} n)} \right]^{1/2}$$
$$\times \left[\frac{(\Omega D_b\delta_b)^7 E}{d^{21}(kT)^{10}} \right]^{1/6} \qquad (37)$$

The nature of the temperature dependence (contained in kT and $D_b\delta_b$) is such that, for typical activation energies ($\approx$400 kJ/mol), the optimum condition for triple-point cavity suppression (i.e. the maximum noncavitating strain rate) should be attained at the highest temperatures.* It is also apparent from Eq. (37) that, as expected,

---

*Testing under conditions suggested by this relation will minimize the tendency for cavity formation when local or applied transients occur during deformation.

fine grain sizes, large boundary diffusivities, and large surface energies permit enhanced noncavitating strain rates to be attained. Some caution should be exercised in applying Eq. (37), because it is confined to the analysis of cavity formation in the region near the triple point. The steady-state cavity nucleation that occurs at grain-facet centers can be analyzed directly from Fig. 9.

Since many practical ceramics contain an amorphous phase at grain triple points, the influence of such phases on cavity nucleation was explored. Viscous flow in the amorphous enclave will rapidly relieve shear stresses that develop as a consequence of sliding. However, the net hydrostatic stress will not be relieved and, if tensile, will tend to nucleate cavities (Eq. (29)). To assess the possible occurrence of hydrostatic tension, the sliding boundaries are simulated by two mode II cracks (Section II). The unrelaxed hydrostatic stress p associated with each crack in plane strain[5] is (Fig. 11):

$$p \equiv (\sigma_{rr} + \sigma_{\theta\theta} + \sigma_{zz})/3 = -0.14(1+\nu)\sigma_\infty \sin(\theta/2)\sqrt{d/x} \qquad (38)$$

For $\theta < 0$, hydrostatic tension develops, whereas for $\theta > 0$ there exists a hydrostatic compression of equal magnitude. The average hydrostatic pressure within a symmetric enclave is thus zero. For example, in a cylindrical enclave, radius r, the average hydrostatic stress $<p>$ is given by:

$$<p> = [0.14(1+\nu)/\pi r^2]\sigma_\infty \int_0^r \sqrt{xd} \int_{-\pi}^{\pi} \sin(\theta/2)d\theta dx = 0 \qquad (39)$$

Symmetric enclaves of an amorphous phase at a triple point should thus be regarded as expedient for the relaxation of stresses by viscous flow, without the concomitant tendency for cavity nucleation. However, the amorphous enclaves in ceramics are rarely symmetric, because of surface-energy anisotropy. Certain asymmetries (e.g. Fig. 11) will result in a net tensile pressure and the enclaves will be potential sites for early cavity nucleation.

The preceding analysis of cavity nucleation implies that attaining appreciable noncavitating strain rates requires fine-grained polycrystals devoid of amorphous phases or grain-boundary precipitates, but with substantial grain-boundary diffusion rates. Additives that encourage grain-boundary diffusion but do not form amorphous phases or grain-boundary precipitates (i.e. solid-solution alloys) must thus be sought, especially additives that do not increase the ratio of the boundary to the surface energy.

(2) Retardation of Cavity Growth

Suppressing cavity formation in ceramics presents stringent fabrication problems, which may prove insurmountable in many instances. The prospects for achieving large strains by retarding cavity growth (i.e. permitting appreciable cavity nucleation) are thus briefly explored. The initial equilibrium growth of the cavities is dictated (Eq. (30)) by the grain-boundary diffusivity $D_b\delta_b$, the surface energy γ_s, and the ratio of the boundary and surface energies. Cavity growth is retarded by large values of γ_s and low ratios of γ_b/γ_s, i.e. requirements consistent with the suppression of cavity nucleation. However, the other requirement for retarding growth, small $D_b\delta_b$, is not compatible with either the attainment of appreciable deformation rates without cavity suppression or the relaxation of internal stress concentrations and cannot be used.[†] The subsequent growth of the cavities which contribute to premature failure involves the development of nonequilibrium shapes; hence, the growth occurs more rapidly for systems with low surface diffusivities or low surface energies (Eq. (31)). Systems with larger surface than boundary diffusivities are thus preferred.

The large surface energy and small boundary energy required to limit premature failure by retarding cavity growth, without depressing the deformation rate, are compatible with the requirements for cavity suppression. The additional requirement for a large relative value of the surface diffusivity suggests that additives which also enhance the relative surface diffusivity should be investigated.

[†]If $D_b\delta_b$ is too small, another deformation mode, such as slip, could replace diffusion creep as the rate-controlling mechanism in the absence of cavity formation. Such a mechanism would tend to encourage fracture.

VI. Conclusion

Studies of the stresses generated by boundary sliding and thermal-expansion anisotropy in the presence of grain-boundary diffusion indicate that large stress concentrations can be averted in fine-grained polycrystals, under conditions which permit relatively rapid diffusional deformation. The stress concentrations can be retained below the level required to nucleate cavities if the boundaries are devoid of low surface-energy amorphous phases and inclusions, especially those with a high interface energy. A brief examination of cavity-growth relations indicates that the surface diffusivity is an additional parameter involved in the high-temperature failure process. A surface diffusivity higher than the boundary diffusivity encourages the equilibrium mode of cavity growth. A search for additives (particularly solid-solution additives) that encourage deformation, while suppressing cavity nucleation or growth, is suggested. The key parameters are a high boundary diffusivity, a small ratio of boundary-to-surface energy, and a rapid surface diffusivity. Little is known about the role of additives on these parameters in ceramic systems. Carefully conceived studies should thus prove fruitful.

APPENDIX I

Elastic Contributions to Void Nucleation

The precise determination of the shape and free energy of formation of a critical-sized nucleus of the type shown in Fig. 6 is a complex problem beyond the scope of the present work. However, to estimate the elastic contributions to the free energy of formation and thus extend previous treatments (where it has been neglected[16]), the exact treatment for a spherical nucleus and approximate treatments for cavities in the shape of a cylinder with an elliptical cross section and for an ellipsoid are presented. The results indicate that the neglect of elastic contributions is usually warranted.

Consider, for simplicity, a body subjected to a hydrostatic tension, $-p$. Production of a vacancy at a dislocation or boundary produces a relaxation energy, $-p\Omega$. At local equilibrium this osmotic force is balanced by a vacancy supersaturation so that the chemical potential of vacancies is equilibrated. Hence:

$$\mu_v - \mu_0 = -p\Omega = kT \ln (C/C_0) \qquad (A-1)$$

where μ_v and μ_0 are the actual and standard-state chemical potentials and C and C_0 are the actual vacancy concentration and the equilibrium concentration in the absence of stress, respectively. Thus for a void containing n vacancies, the reversible work term (Helmholtz free energy) associated with vacancy removal is

$$\Delta F_1 = -pV \qquad (A-2)$$

where $V = n\Omega$ is the volume of the void.

In addition, for a spherical void in an isotropic elastic solid, there will be an "image" relaxation, giving an added elastic contribution to ΔF. Consider cutting a spherical hole in a continuum, adding image stresses $-\sigma_{rr}$ to establish a force-free boundary, and relaxing. This problem is standard for elasticity and gives a stress

$$\sigma_{rr} = -(G\delta v/\pi r_0^3) \qquad (A-3)$$

with r_0 the initial radius of the void and δv the relaxation volume. Since σ_{rr} at $r_0 = -p$,

$$\delta v = \pi r_0^3 p/G \qquad (A-4)$$

The outer free surface will expand more (by a factor $(1 + 4G/3B)$), with B the bulk modulus. Hence the added work term is

$$\Delta F_2 = -p^2 \pi r_0^3 (1 + 4G/3B)/2G = 3p^2 V (1 + 4G/3B)/8G \qquad (A-5)$$

For typical stresses $p \lesssim 10^{-3}G$, ΔF_2 is $\leq 0.1\%$ of ΔF_1 and hence negligible.

More dramatically, to the linear elastic approximation of considering vacancies as tiny spherical holes, the relaxation of the type

giving ΔF_2 will have already been produced when the vacancies form and the added relaxation when the vacancies cluster to form a void would be zero. Even in a nonlinear model, the tendency will always be for part of ΔF_2 to accompany vacancy formation and reduce the contribution to void-free energy (except for the unusual case of aluminum where a vacancy appears to be a center of compression on the basis of experimental measurements of vacancy concentration as a function of pressure).

In the case of uniaxial tension, ΔF_2 could, in principle, be more important. This possibility occurs because a void of given volume could spread into a disk shape, with the plane of the disk normal to the uniaxial force, and produce greater relaxation of external force than in the spherical-void case (the classic Eshelby-Nabarro result). For small particles, this tendency will be opposed by surface energy. Hence, the problem is to determine the equilibrium shape of a void of given size. To examine this possibility, consider (for mathematical simplicity) the two-dimensional problem of a right-circular cylinder void relaxing to one of elliptical cross section. The exact solution is a complicated variational problem and only an approximate solution can be obtained analytically. However, in the present case, the regime of interest can be described by limiting procedures.

For uniaxial stress σ, if vacancies are created at dislocations with Burgers vectors parallel to the applied force or at boundaries lying normal to the force, the chemical balance gives

$$\mu_v - \mu_0 = \sigma\Omega \qquad (A-6)$$

$$\Delta F_1 = \sigma V \qquad (A-7)$$

For a cylinder, the equivalent work term to Eq. (A-5) is

$$\Delta F_2 = -3[\sigma^2 (1 - \nu^2)\pi a^2/2E] \qquad (A-8)$$

where a is the cylinder radius and ν is Poisson's ratio. As in the linear elastic case, the work ΔF_2 is already included in vacancy formation. Any added contribution to the void-formation energy will thus be that of relaxing the cylinder to an ellipse.

An exact solution would involve equilibrating the local chemical potential of an atom at the surface as influenced by curvature with that associated with local strain-energy density w, i.e.

$$\mu - \mu_0 = \gamma\Omega/r = w\Omega \qquad (A-9)$$

An exact solution is difficult because both r and w depend (differently) on cylindrical coordinates fixed on the center of the hole. Hence, the general minimization is a complicated variational problem. To gain insight into the solution, the simpler problem of a fixed class of shape is treated, i.e. an elliptical hole with major and minor axes x and y, with uniaxial tensile stress giving a tensile force acting parallel to y.

The relaxational strain energy of an elliptical hole is given by Rice[7] as

$$\Delta F_3 = -(A/2)[\sigma^2 (1 - \nu^2)/E][1 + 2(x/y)]^2 \qquad (A-10)$$

where $A = \pi xy$ is the cross-sectional area for unit length of the cylinder. The corresponding surface-energy term is

$$\Delta F_4 = \pi\gamma(x+y)\left[1 + {}^1/_4 \left(\frac{x-y}{x+y} \right)^2 + {}^1/_{64} \left(\frac{x-y}{x+y} \right)^4 + \ldots \right] \qquad (A-11)$$

The simpler variational problem is then to minimize $(\Delta F_3 + \Delta F_4)$ with respect to x and with $A = \pi xy$ held constant. An expansion to first order in $(x - y)$, with the validity to be checked a posteriori gives

$$(x - y)/x = [4\sigma^2 (1 - \nu^2)/3E(\gamma/b)](x/b) \qquad (A-12)$$

For typical values $\sigma/E = 10^{-3}$, $\nu = 1/3$, and $\gamma/bE = 2 \times 10^{-2}$, the result is

x/b:	1	10^2	10^3
$(x-y)/x$:	5×10^{-5}	5×10^{-3}	0.05

Thus, since $b \approx 2 \times 10^{-10}$ m is an atomic dimension, the deviation of

the ellipse from sphericity is essentially negligible until $x \geqslant 0.1$ μm. Correspondingly, the shape-change energy relaxation is negligible compared to the already small ΔF_2 until $x \geqslant 0.1$ μm. Typical critical-sized nuclei when nucleation is appreciable (see text) vary from $x = 0.1$ to 10 nm. Thus, in the range of interest for nucleation, the expansion leading to Eq. (A-12) is accurate and shows that the elastic shape relaxation term is negligible. In void growth after nucleation, this elastic term will become important for sizes above $x \cong 0.1$ μm. In this case, higher-order terms in Eqs. (A-10) and (A-11) would be required to give the solution equivalent to Eq. (A-12).

The preceding discussion treated a homogeneous void within a grain. For a lens-shaped void at a boundary, the relative importance of the elastic terms will be unchanged for the hydrostatic pressure case where the contact angle will be a function of relative surface energies only and curvature will depend only on the hydrostatic stress, p. For the normal stress, the elastic stress concentration at the point of contact with the boundary will differ from that of the internal void. However, in view of the two-orders-of-magnitude difference between the size range of interest and the actual size as reflected in the earlier result it is unlikely that the added stress would shift the important size regime for appreciable contributions of the elastic term into the nucleation-size regime. To formally treat the boundary case, a fixed-shape class could not be assumed; rather, the full variational treatment would be needed.

As a final estimate of elastic terms, the double cap-shaped lens of Fig. 6 was approximated by an ellipsoid with major and minor axes x and y, respectively, and with $x = r$ $\sin\alpha$ (to correspond to Fig. 6) was assumed. Sneddon[21] gives the energy term equivalent to Eq. (A-5) for such a case (but in an infinite medium with uniaxial stress giving a tensile force parallel to y) as

$$\Delta F_5 = [8(1 - \nu^2)\sigma^2 x^3 / 3E] \tag{A-13}$$

As in the previous cases, part of the relaxation energy is already associated with vacancy formation. Also, diffusive motions in adjoining material may act to reduce local stresses[6,13] so that the elastic energy changes are yet smaller. Both of these factors are included in the analysis by introducing a factor β into Eq. (A-13) with $0 < \beta \leqslant 1$. This form is used in the text.

APPENDIX II

Boundary Energies in Ceramics

The frequent occurrence of transgranular, rather than intergranular, fracture in many ceramic polycrystals would imply that the energies of a substantial proportion of the boundaries are quite low. Although it is recognized that fracture energies cannot be equated to thermodynamic energies, it is reasonable to anticipate that the ratio of the boundary fracture energy, γ_{fb}, to the transcrystalline fracture energy, γ_{fc}, should reflect the relative values of the boundary and surface energies, through the relation[5]

$$\gamma_{fb}/\gamma_{fc} = (2\gamma_s - \gamma_b)/2\gamma_s \tag{A-14}$$

or

$$\gamma_b/2\gamma_s = 1 - (\gamma_{fb}/\gamma_{fs}) \tag{A-15}$$

A crack will propagate transgranularly if the stress intensity factor for extension along the preferred cleavage plane exceeds the crystalline crack-extension resistance, before the stress intensity factor for extension along the boundary exceeds the boundary crack-extension resistance. The maximum probability of transgranular crack extension in a polygon array (Fig. 1) occurs when the cleavage plane is coplanar with the crack plane ($\theta = 0$) and the boundary inclination is $\pi/3$. This condition thus yields a lower limit for the ratio of the boundary to the cleavage fracture resistance in materials that exhibit some transgranular fracture.

Recent solutions for the angled crack[22] indicate that the stress intensity factor ratio along the plane $\theta = 0$ and $\pi/3$ is ≈ 1.54. Hence, $\gamma_{fb} > 0.42$ γ_{fc} and, from Eq. (A-15), $\gamma_b < 1.2\gamma_s$ for transgranular cracking to occur. However, the possibility that some boundaries have larger energies cannot be excluded.

References

[1] R. L. Coble; p. 200 in W. D. Kingery, H. K. Bowen, and D. R. Uhlmann, Introduction to Ceramics, 2d ed. Wiley & Sons, New York. 1976.

[2] F. F. Lange; unpublished work.

[3] A. G. Evans, R. L. Coble, and R. M. Cannon, Preliminary Reports, Memoranda and Technical Notes of the DARPA Materials Research Council, University of Michigan, Ann Arbor, Mich., 1976.

[4] C. W. Lau and A. S. Argon; pp. 595–601 in Fracture 1977, Vol. 2. Edited by D. M. R. Taplin. University of Waterloo Press, Waterloo, Ontario, Canada, 1977.

[5] B. R. Lawn and T. R. Wilshaw, Fracture of Brittle Solids. Cambridge University Press, London, England, 1976.

[6] T.-J. Chuang, "Models of Intergranular Creep Crack Growth by Coupled Crack Surface and Grain Boundary Diffusion," Univ. Microfilms Int. (Ann Arbor, Mich.) Order No. 76–15618. 95 pp.; Diss. Abstr. Int. B, 37 [1] 402 (1976).

[7] J. R. Rice; pp. 191–311 in Fracture, Vol. II. Edited by H. Liebowitz. Academic Press, New York, 1968.

[8] R. M. Cannon and R. L. Coble; pp. 61–100 in Deformation of Ceramic Materials. Edited by R. C. Bradt and R. E. Tressler. Plenum, New York, 1975.

[9] R. M. Cannon; private communication.

[10] R. Raj and M. F. Ashby, "Grain Boundary Sliding and Diffusional Creep," Metall. Trans., 2 [4] 1113–27 (1971).

[11] T.-J. Chuang, K. I. Kagawa, J. R. Rice, and L. B. Sills. "Non-Equilibrium Models for Diffusive Cavitation of Grain Interfaces," Acta Metall., 27 [3] 265–84 (1979).

[12] R. Raj, "Crack Initiation in Grain Boundaries Under Conditions of Steady-State and Cyclic Creep," J. Eng. Mater. Technol., 98 [2] 132–39 (1976).

[13] A. G. Evans, "Microfracture from Thermal Expansion Anisotropy: I", Acta Metall., 26 [12] 1845–53 (1978).

[14] D. C. Drucker; p. 795 in High Strength Materials. Edited by V. F. Zackay and E. R. Parker. Wiley & Sons, New York, 1965.

[15] R. Raj, "Intergranular Fracture in Bicrystals," Acta Metall., 26 [2] 341–49 (1978).

[16] R. Raj and M. F. Ashby, "Intergranular Fracture at Elevated Temperatures," ibid. 23 [2] 653–66 (1975).

[17] J. P. Hirth and G. M. Pound, Condensation and Evaporation (Progress in Materials Science, Vol. 11); p. 162. Edited by B. Chalmers and R. King. Pergamon, New York, 1963.

[18] B. K. Chakraverty and G. M. Pound, "Heterogeneous Nucleation at Macroscopic Steps," Acta Metall., 12 [8] 851–60 (1964).

[19] J. Feder, K. C. Russell, J. Lothe, and G. M. Pound, "Homogeneous Nucleation and Growth of Droplets in Vapors," Adv. Phys., 15 [57] 111–78 (1966).

[20] R. L. Coble, "Model for Boundary Diffusion Controlled Creep in Polycrystalline Materials," J. Appl. Phys., 34 [6] 1679–82 (1963).

[21] I. N. Sneddon, Fourier Transforms; p. 486. McGraw-Hill, New York, 1951.

[22] B. A. Bilby, G. E. Cardew, and I. C. Howard; pp. 197–200 in Fracture 1977, Vol. 3. Edited by D. M. R. Taplin. University of Waterloo Press, Waterloo, Ontario, Canada, 1977.